Available online at www.sciencedirect.com

SciVerse ScienceDirect

Procedia Environmental Sciences 10 (2011) 178 – 184

Procedia Environmental Sciences

2011 3rd International Conference on Environmental Science and Information Application Technology (ESIAT 2011)

Numerical Simulation of the Direct Effects on Climate in East Asia Induced by Carbonaceous Aerosol

Xinmei Chen and Jian Wu*

Department of Atmospheric Science, Yunnan University, Kunming, 650091, P. R. China

Abstract

Carbonaceous aerosol is one of the main ingredients of the atmospheric aerosol, which includes black carbon and organic carbon. The numerical simulations from 1960 to 2000 are aimed at the direct radiative effects on climate induced by carbonaceous aerosol in East Asia using NCAR Community Atmospheric Model version 3.1 (CAM). The mean radiative forcing(RF) under all sky in Chinese mainland at TOA and surface are 0.38 and -5.31W/m^2 respectively. This distinct RF leads to -0.1K surface temperature decrease in Chinese mainland, which includes -0.26K drop of daily maximum and 0.07K rise of minimum temperature. Air column temperature has also been increased 0.11K in Chinese mainland. Significant vapor and precipitation increase can be resulted from RF of carbonaceous aerosol in north China and the Yellow and Huai River basin, accompanied by the decrease in northeast China, far-east region, and Tibet Plateau.

Keywords: Carbonaceous aerosol; Direct effects; Climate change; Numerical simulation; East Asia

1. Introduction

Carbonaceous aerosol, including black carbon (BC) and organic carbon (OC), is one of the ingredients of the atmospheric aerosol. It comes from both anthropogenic and natural origins including incomplete combustion of carbon fuel and biomass burning. Carbonaceous aerosol emission inventories suggest that approximately 34 to 38% of emissions come from biomass burning sources and the remainder from fossil fuel burning sources. According to the inventory of carbonaceous aerosol in 1996, the total emission

*Corresponding author
E-mail address: wujian@ynu.edu.c n

doi:10.1016/j.proenv.2011.09.031

mount of BC and OC was 8.0Tg and 34Tg respectively, and both of them are decreasing in terms of the prediction of carbonaceous emission under IPCC scenarios (Streets, 2004).

The radiative characteristics of BC includes both of absorption and scattering, while OC shows much more scattering than that of BC (d'Almeida, 1991). Now the sign of carbonaceous aerosol's RF is still in question (Forster, 2007), which refers to the change of net downward radiation fluxes induced by aerosol or green house gases. For some simulation results, the fossil fuel BC RF ranges from 0.15 to 0.27Wm^{-2} with a mean of 0.25Wm^{-2}. The mean and median of the direct RF for biomass burning aerosol from grouping all recent simulations are similar at 0.04 and 0.02Wm^{-2} (Forster, 2007). The biomass burning aerosol includes OC, BC and inorganic compounds such as nitrate and sulfate. According to the samples collected in Shanghai China, carbonaceous aerosol accounts for 41.6% of the PM 2.5 mass, with 73% of that mass being organic (Ye, 2003). The climate responses of carbonaceous aerosol are investigated by simulations (Jacobson, 2004), and it reveals the near-surface temperature change about 0.27K.

In recent years, changes of precipitation in China have been observed, and there are distinctive regional and seasonal patterns (Zhai, 2005), especially for the significantly decrease of annual total precipitation in northeast China, north China, and central west China, accompanied by the increase in South China, central east China, and west China (Ding, 2007). The potential relation between aerosol and the trend of precipitation has also been explored in some simulations. Some simulations are inclined to relate the changes of precipitation in East Asia to the effects of BC (Menon, 2002; Ramanathan, 2005; Wu, 2004; Wu, 2008). On the contrary, Gu (2006) investigated different types of aerosol and stressed that the inclusion of black carbon in their simulations did not produce the "north drought/south flooding" precipitation pattern occurred frequently in China during the past 50 years.

These well-designed simulations and some observation analysis improved our understanding in carbonaceous aerosol's climatic effects, while it also needs further research. In this work, the NCAR Community Atmospheric Model version 3.1 (CAM) is used to estimate the direct effects of carbonaceous aerosol, and the change of temperature and precipitation in East Asia.

The paper is organized as following. The model and simulation strategy is described in section 2. Section 3 describes the results of RF, and the change of temperature and precipitation induced by carbonaceous aerosol. Conclusions and discussions are given in section 4.

2. Model, simulation strategy, and data

The NCAR Community Atmospheric Model version 3.1 is at T42 spectral truncation (roughly 2.8°×2.8° horizontal resolution) and has a 26-level hybrid sigma-pressure coordinate system (Collins, 2004). The model is driven by time-dependent monthly mean sea-surface temperature (SST), and sea-ice concentration dataset (Hurrell, 2006).

Two different CAM integrations from 1960 to 2000 are performed with the spin-up time of the first 10 years. The control simulation (CN) includes the forcing from carbonaceous aerosol and sea salt, and the aerosol simulation (AR) only includes the forcing from sea salt. The same parameters are used in the two experiments. The concentrations of greenhouse gases are held constant at 1990 levels. To analyze the effects of total combined aerosol on climate, the 30-year mean simulations from the CN experiment are compared to that of AR.

The three-dimensional time-dependent distributions of carbonaceous aerosol are included in the model with the prescribed dataset. The aerosol dataset comes from an aerosol assimilation system (Collins et al., 2001, 2002) integrated for present-day condition, in which the Model for Atmospheric Chemistry and Transport (MATCH) (Rasch et al., 1997) and an assimilation of satellite retrievals of aerosol optical depth are used including anthropogenic and natural sources for aerosol. The direct effects of tropospheric aerosols on solar fluxes and heating rates are included, and indirect effects are not included in the model.

The carbonaceous optical depth used in the simulation is shown by figure 1. Its high value region lies in east and south China with maximum of 0.06 in Sichuan basin and the middle reaches of the Yangtze River. It is below 0.02 in north China. The lowest value locates in Tibet Plateau and northwest China.

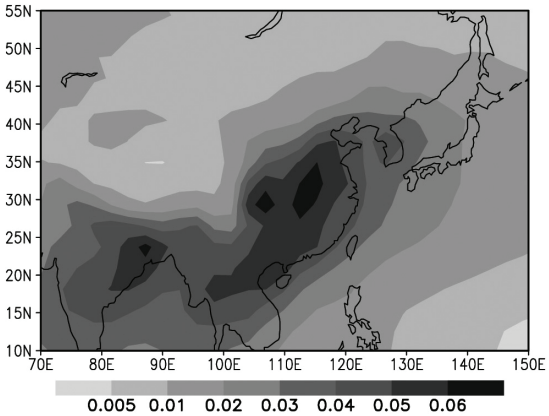

Figure 1. Annual mean optical depth of carbonaceous aerosol at 550nm used in the simulations

3. Radiative forcing and climate change

The RF at top of the atmosphere (TOA) is positive in southeast China with maximum value of 2W/m^2, and it reaches the highest at Tibet Plateau of 6W/m^2 (Figure 2a). In other areas, the RFs are negative with the lowest value of -6W/m^2 over the Bengal Sea.

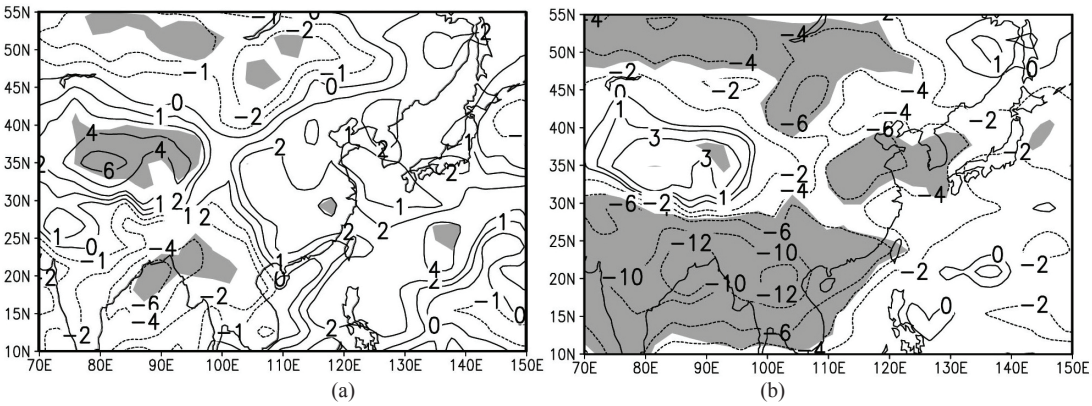

Figure 2. Annual mean RF at TOA(a) and surface(b) under all sky (unit: W/m^2; contour) and regions passing significance t-test at 90% confident level (shade)

Compared to figure 1, the regions of negative RF are of lower optical depth. The negative RF results from the scattering effects of carbonaceous aerosol. The positive RF in southeast China agrees well with the high optical depth region shown by figure 1, and it should be related to the multi-reflection effects among aerosol particles, which can enhance the absorption to radiation of the air column among aerosol. The positive RF on Tibet Plateau, with lower optical depth and higher surface albedo, should be deduced

to the absorption increase of the air column between surface and aerosol layer induced by multi-reflection between them.

The RFs at surface are almost negative with the most significant value of -12W/m^2 over Indo-China Peninsula (Figure 2b). Compared to figure 2a, the RFs at surface in southeast China and the middle and low researches of the Yangtze River are negative, which infers the enhancement of atmospheric absorption in the region. There also exists positive RF over Tibet Plateau in figure 2b, but it is not statistically significant.

Change of surface temperature is one of the results induced by aerosol RF. Distinct decrease of surface temperature can be found in India and southwest China with the most remarkable value of 0.5K (Figure 3a). The surface temperature is increased in north China and Tibet Plateau below 0.2K, accompanied by weak decrease in the Yellow and Huai River basin and the middle reaches of the Yangtze River. The mean changes of surface temperature is -0.1K in Chinese mainland, -0.03K in north China, -0.06K in south China, -0.25K in southwest China, and 0.03K in northwest China respectively. The pattern of surface temperature drop agrees well with that of RF at surface.

Because carbon aerosol can scatter much solar radiation in day time and absorb infrared radiation emitted by the surface in night time, the temperature range should be changed. The monthly mean range of surface temperature is decreased in most part of the model domain except Tibet Plateau (Figure 3b). It can exceed -1K in most part of south to the Yellow River with the lowest value of -1.6K in the Yellow and Huai River basin and Sichuan basin, but it is not statistically significant. The decrease of monthly range of surface temperature is also distinct in north China and Mongolia, east and north India.

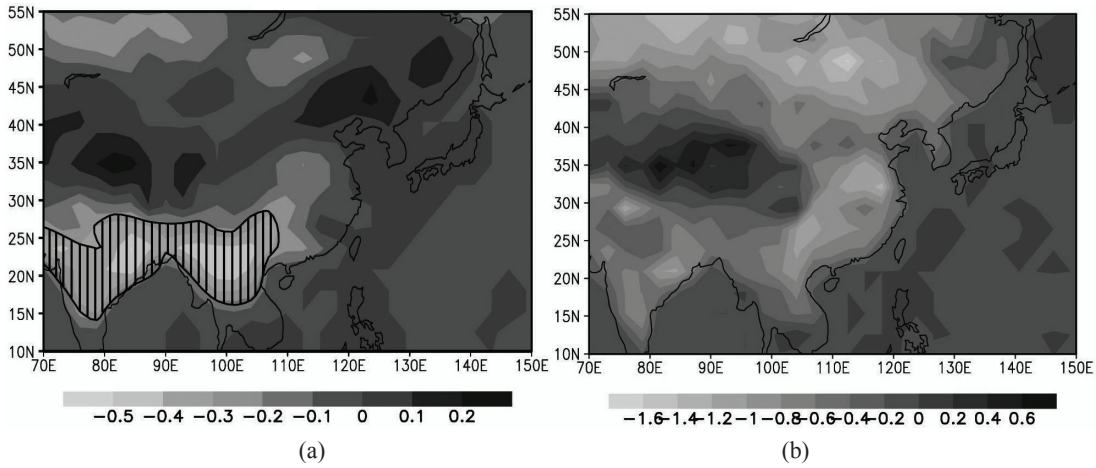

Figure 3. (a) Change of surface temperature (unit: K, shade) and regions passing significance t-test at 90% confident level (strip line); (b) change of monthly range of surface temperature (unit: K)

In addition, changes of air temperature in different air pressure levels are shown in figure 4a. For the four investigated regions, the changes of air temperature are much more distinct near the surface and the tropopause, while it is weaker in the middle of troposphere. The most distinct temperature drop lies in southwest China with significant value close to -0.2K near the surface. Temperature rises can be found in north, south, northwest China in most part of troposphere with maximum of 0.25K in north China. The significant temperature increase results from the excessive absorption to solar radiation induced by carbonaceous aerosol. The stabilities of air column below 300hPa become more stable in south, northwest, and southwest China, due to the much bigger rise of temperature in higher levels than that of lower levels.

It has reverse trends in the levels between 700-900hPa in north China, and layers between 200-300hPa for the four regions.

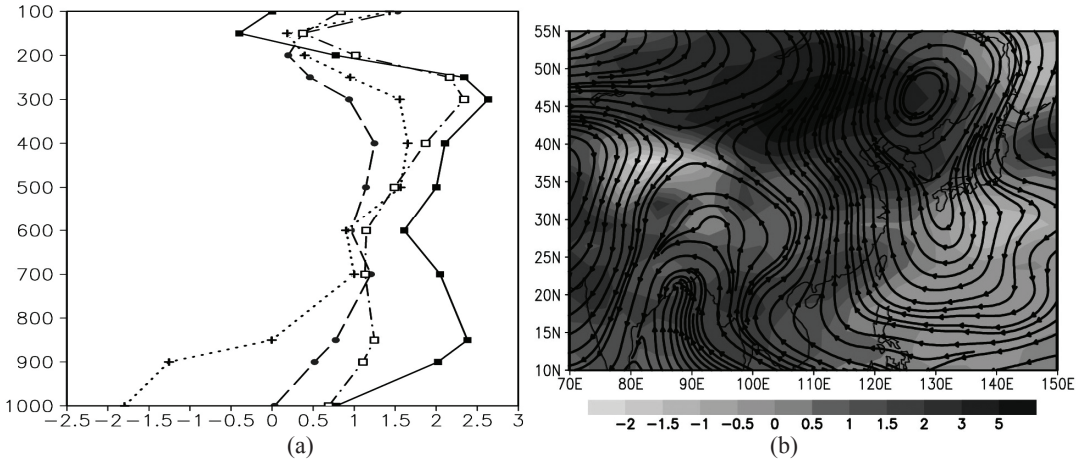

Figure 4. (a) Change of air temperature profiles in the four investigated regions (unit: 0.1K; solid: north China, dashed: south China, dot: southwest China, dashed and dot: northwest China); (b) Percentage changes of vapor column burden (shade) and vapor flux change below 500 hPa (streamline) averaged over the simulation period

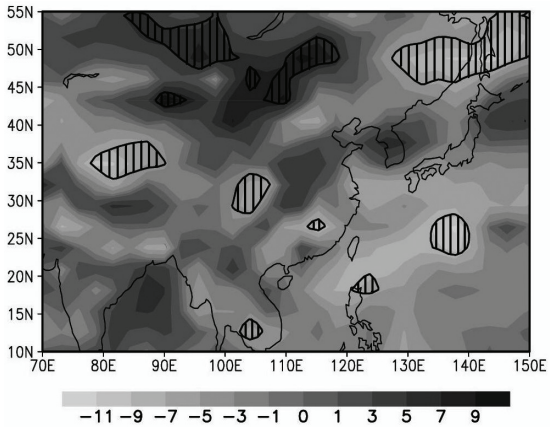

Figure 5. Percentage changes of total rainfall averaged over the simulation period (shade) and regions passing significance t-test at 90% confident level (strip line)

The change of temperature can disturb the air pressure, which in turn leads to the change of stream. The percentage change of vapor column burden is shown in figure 4b. Vapor increase regions include south China, the Yellow and Huai River basin, north China, accompanied by the decreases in the middle of Chinese mainland, Sichuan basin and Tibet Plateau. The notable vapor increase can exceed 2% in south edge of south China, north China, with maximum of 5% in north China. The significant vapor decrease region lies in Tibet Plateau with the lowest value of -2%.

The pattern of vapor streamline includes two anti-cyclones in west and east of the domain, and two cyclones in south and north of the domain respectively. The south wind in west edge of the biggest anti-cyclone, located in east part of the domain, accords for the vapor increase in north China. The belt of

vapor increase in south China results from the south wind in the west edge of biggest anti-cyclone and in the east edge of the cyclone bow, located in the Bengal Bay. The decrease of vapor in Tibet Plateau is mainly due to the north wind at the west edge of the anti-cyclone over India, in which the dryer air mass is transported. The averaged vapor content in Chinese mainland is increased 1.1%, accompanied by the increase of 1.53%, 0.85%, 1.17%, and 0.96% in north, south, southwest, and northwest China respectively.

As an important aspect of climate changes, change of precipitation is also induced by carbonaceous aerosol. The weak decrease of precipitation in some parts of south and north China is revealed by figure 5, and the distinct drop of rainfall lies in Tibet Plateau, Far-east regions, and the west Pacific Ocean with lowest value of -11%, which can pass the significance t-test. Precipitation increase can be found in Mongolia, north China, the Yellow and Huai River basin, southwest China, and the Bengal Bay, in which the most remarkable value can reach 7-9%. The regions of rainfall increase fail to pass the significance t-test.

4. Conclusion

The direct radiative effects of carbonaceous aerosol in East Asia have been explored using CAM3.1. Its RF and climate changes have been discussed. The main conclusions are as follows:

[1] RF at TOA induced by carbonaceous aerosol is negative in north China, southwest China, but it's positive in the middle and southeast China, and Tibet Plateau. RF at the surface is negative except in the Tibet Plateau with the extreme value of -12W/m^2.

[2] Surface temperature deceases distinctly in south China with the lowest value of -0.5K, while it rises weakly in north China and Tibet Plateau. The monthly range of surface temperature drops significantly in the most part of the domain except Tibet Plateau. Air temperature below 300hPa level increases in south, northwest, southwest China.

[3] Water vapor is increased in most regions of Chinese mainland, which leads to the rise of precipitation in north China, the Yellow and Huai basin. Vapor decrease can be found in Tibet Plateau, Sichuan basin, and Far-east region, which is in a good agreement with the decrease of rainfall.

In our simulation, the indirect effects of carbonaceous aerosol have not been included, which is also important to climate change. The effects of atmosphere to ocean have been excluded in this simulation by the prescribed SSTs, which would distort the results and should be considered in further work.

Acknowledgements

The study was sponsored by the National Natural Science Foundation of China (40975092), the Natural Science Foundation (2009CD021) and the Foundation of Younger Scholars in Science and Technology (2009CI046) of Yunnan Province.

References

[1] Streets, D. G., T. C. Bond, T. Lee, C. Jang. On the future of carbonaceous aerosol emissions, *J. Geophys. Res.*, 2004, **109**, D24212, doi:10.1029/2004JD004902.

[2] d'Almeida, G.A., P. Koepke, E.P. Shettle. Atmospheric Aerosol: Global Climatology and Radiative Characteristsics, A. Deepak, Hampton, Va., 1991.

[3] Forster, P., V. Ramaswamy, P. Artaxo, T. Berntsen, R. Betts, D.W. Fahey, et al. *Changes in Atmospheric Constituents and in Radiative Forcing. In: Climate Change 2007: The Physical Science Basis.* Contribution of Working Group I to the Fourth Assessment Report of the Intergovernmental Panel on Climate Change [Solomon, S., D. Qin, M. Manning, Z. Chen, M. Marquis, K.B. Averyt, M.Tignor and H.L. Miller (eds.)]. Cambridge University Press, Cambridge, United Kingdom and New York, NY, USA, 2007.

[4] Ye, B., X. Ji, H. Yang, X. Yao, C. K. Chan, S. H. Cadle, et al. Concentration and chemical composition of $PM_{2.5}$ in Shanghai for 1-year period. *Atmos. Environ*., 2003, **37**: 499-510.

[5] Jacobson, M. Z.. Climate response of fossil fuel and biofuel soot, accounting for soot's feedback to snow and sea ice albedo and emissivity, *J. Geophys. Res.*, 2004, **109**, D21201, doi:10.1029/2004JD004945.

[6] Zhai, P., X. Zhang, H. Wan, X. Pan, Trends in total precipitation and frequency of daily precipitation extremes over China, *J. Climate*, 2005, **18**: 1096-108.

[7] Ding, Y., G. Ren, G. Shi, P. Gong, X. Zheng, P., et al. China's National Assessment Report on Climate Change (I): Climate change in China and the future trend, *Adv. Clim. Change Res.*, 2007, **3**, 1-5.

[8] Menon, S., Hansen, J., Nazarenko, L., Y. Luo. Climate effects of black carbon aerosols in China and India. *Science*, 2002, **297**, 2250-3,doi:1126/science.1075159.

[9] Ramanathan, V., C. Chung, D. Kim, T. Bettge, L. Buja, J.T. Kiehl, et al. Atmospheric brown clouds: Impacts on South Asian climate and hydrological cycle, *Proc. Natl. Acad. Sci.*, 2005, **102(15)**:5236-333, doi:10.1073/pnas.0500656102.

[10] Wu J., W. M. Jiang, C. B. Fu, B.K. Su, H. N. Liu, J. P. Tang. Simulation of the radiative effect of black carbon aerosols and the regional climate responses over China. *Adv. Atmos. Sci.*, 2004, **21(4)**: 637-49.

[11] Wu J., C. Fu, Y. Xu, J. P. Tang, W. Wang, Z. Wang, Simulation of direct effects of black carbon aerosol on temperature and hydrological cycle in Asia by a regional climate model, *Metero. Atmos. Phys.*, 2008, **100**:179-193.

[12] Gu, Y., K. N. Liou, Y. Xue, C. R. Mechoso, W. Li, Y. Luo. Climatic effects of different aerosol types in China simulated by the UCLA general circulation model, *J. Geophys. Res.*, 2006, **111**, D15201, doi:10.1029/2005JD006312.